Electronic Supplementary Material (ESI) for Materials Advances.

Supporting Information

Beyond Acid Treatment of PEDOT:PSS: Decoding Mechanisms of Electrical Conductivity Enhancement

Hatef Yousefian[a], Seyed Alireza Hashemi[a], Amin Babaei-Ghazvini[b], Bishnu Acharya[b], Ahmadreza Ghaffarkhah[a,*], Mohammad Arjmand[a,*]

[a]*Nanomaterials and Polymer Nanocomposites Laboratory, School of Engineering, University of British Columbia, Kelowna, BC, V1V 1V7, Canada*

[b]*Department of Chemical and Biological Engineering, University of Saskatchewan, 57 Campus Drive, Saskatoon, SK S7N 5A9, Canada*

Corresponding authors: *ah.ghaffarkhah@ubc.ca*, *mohammad.arjmand@ubc.ca*

1. GIWAXS measurements

The average number of packed PEDOT chains in the nanocrystal, as described in the main manuscript, was calculated as follows:[1]

$$N_{avg} = \left(\frac{CCL_{q_{xy}}}{d} \times \frac{E\%}{E\% + F\%}\right) + \left(\frac{CCL_{q_z}}{d} \times \frac{F\%}{E\% + F\%}\right) \quad \text{(S1)}$$

where CCL_{qxy} and CCL_{qz} represent the in-plane and out-of-plane correlation length of the crystal, E% and F% represent edge-on and face-on fraction in the film, and d represents the π-π distance of the packed PEDOT chains.

2. EMI shielding measurements and setup

EMI shielding characteristics of fabricated films were assessed within the X-band frequency range (8.2-12.4 GHz) using a vector network analyzer (VNA) (P9374A Keysight) equipped with a WR90 waveguide. The micrometer thick conductive PEDOT:PSS films were first attached to an offset short and sandwiched between waveguide adaptors. Thence, the samples were exposed to signals within the X-band frequency range, and the shielding parameters were calculated according to the complex scattering (S-) parameters.[2] By considering the complex S-parameters, the reflectance (R), transmittance (T), and absorbance (A) were measured via the following formulations:

$$R = {S_{11}}^2 \quad \text{(S2)}$$

$$T = {S_{21}}^2 \quad \text{(S3)}$$

$$A = 1 - R - T \quad \text{(S4)}$$

where S_{11} is the divided reflected voltage magnitude over the incident voltage magnitude in port S_1, whereas S_{21} is the transmitted voltage magnitude from port 1 to port 2 divided by the incident

voltage magnitude in port 1. Other shielding parameters, including EMI reflection loss (SE_R) and absorption loss (SE_A), were measured as follows:

$$SE_R = 10 \log \left(\frac{1}{1-R}\right) \quad \text{(S5)}$$

$$SE_A = 10 \log \left(\frac{1-R}{T}\right) \quad \text{(S6)}$$

The total EMI shielding effectiveness (SE_T) is measured by the sum of SE_R and SE_A, i.e., $SE_T = SE_R + SE_A$. The specific shielding effectiveness (SSE/t) of shields was calculated by the following equation:

$$SSE/t = \frac{SE_T}{\rho * t} \quad \text{(S7)}$$

in which t is the thickness of the sample in cm, and ρ represents the density in $g.cm^{-3}$. This parameter considers the lightness and SE_T of a sample simultaneously, giving a critical insight into the practicality of the shield for weight-wise applications.

3. Figures

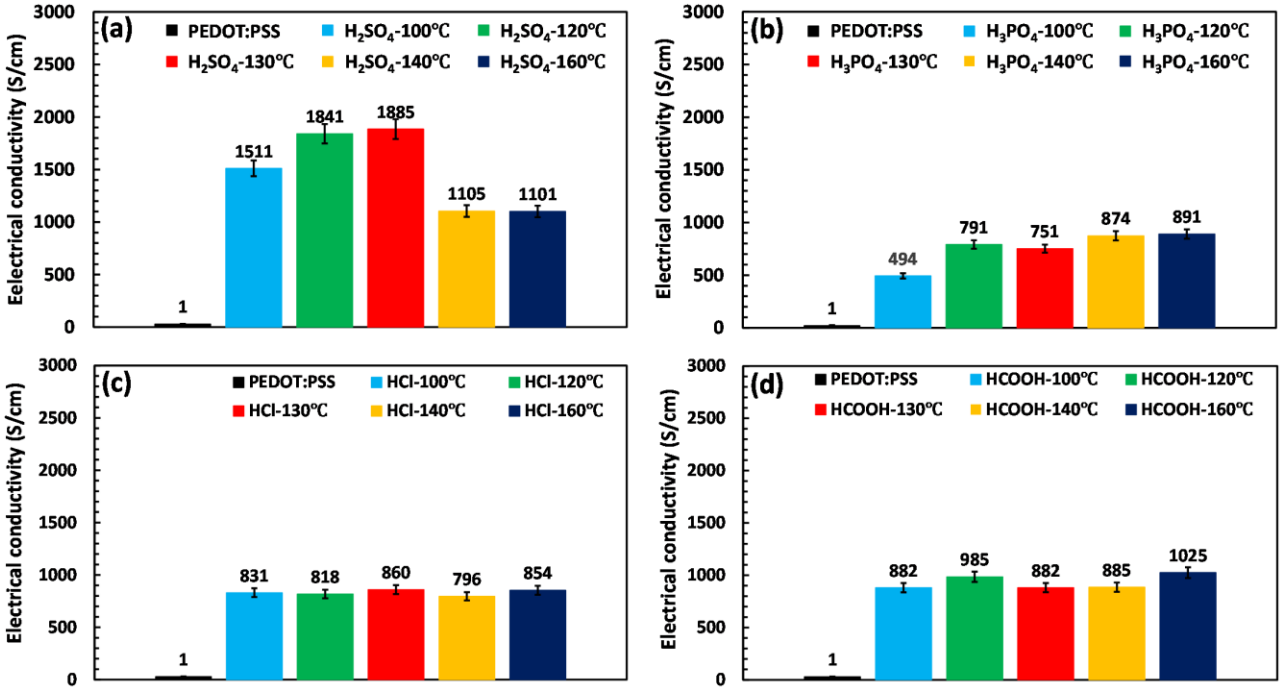

Fig. S1 Electrical conductivity of PEDOT:PSS after a) H_2SO_4, b) H_3PO_4, c) HCl, and d) HCOOH post-treatment at different annealing temperatures.

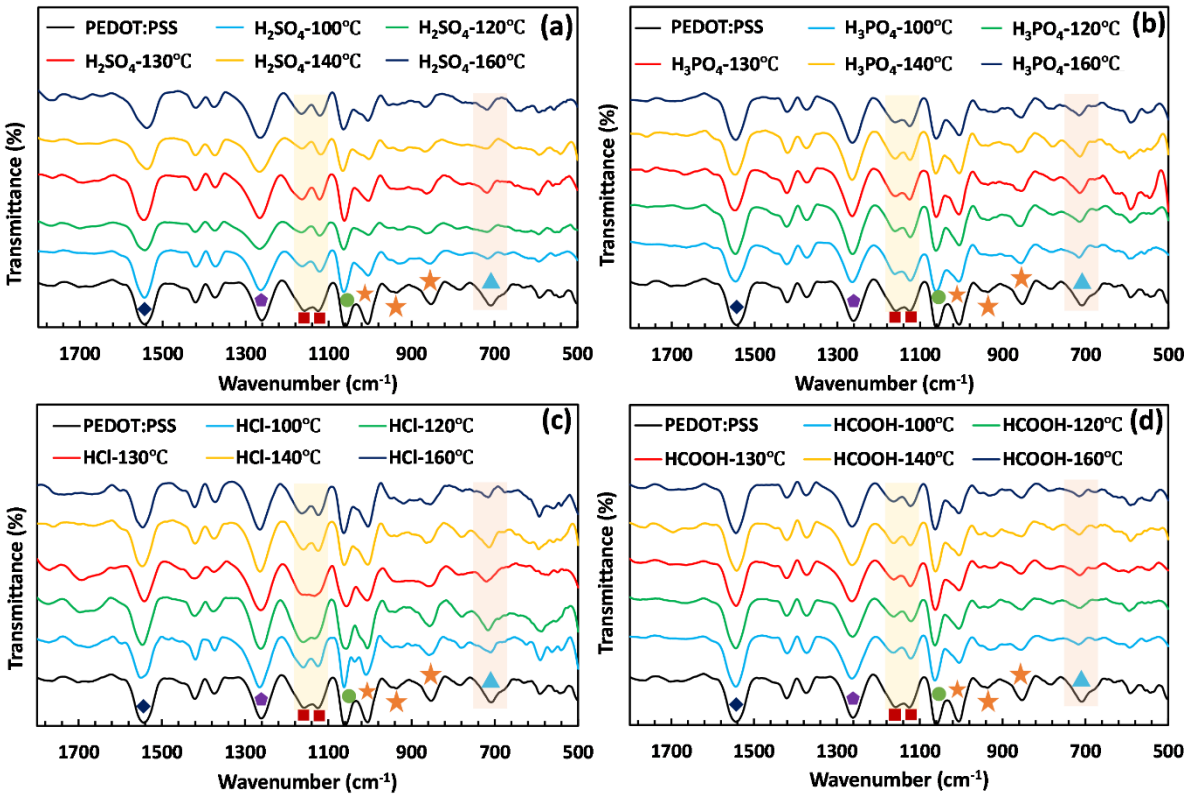

Fig. S2 FTIR analysis of PEDOT:PSS treated at the different annealing temperatures with a) H_2SO_4, b) H_3PO_4, c) HCl, and d) HCOOH. The symbols in Fig. S2 represent the assigned peaks of FTIR analysis. The orange star, dark blue diamond, and purple hexagon are attributed to $C-S$, $C-C$ and $C=C$ bonds of PEDOT, respectively. The $C-S$ bond, S-phenyl group, and symmetric/asymmetric stretching vibrations of SO_3^- groups of PSS are shown by the blue triangle, green circle, and red square, respectively.

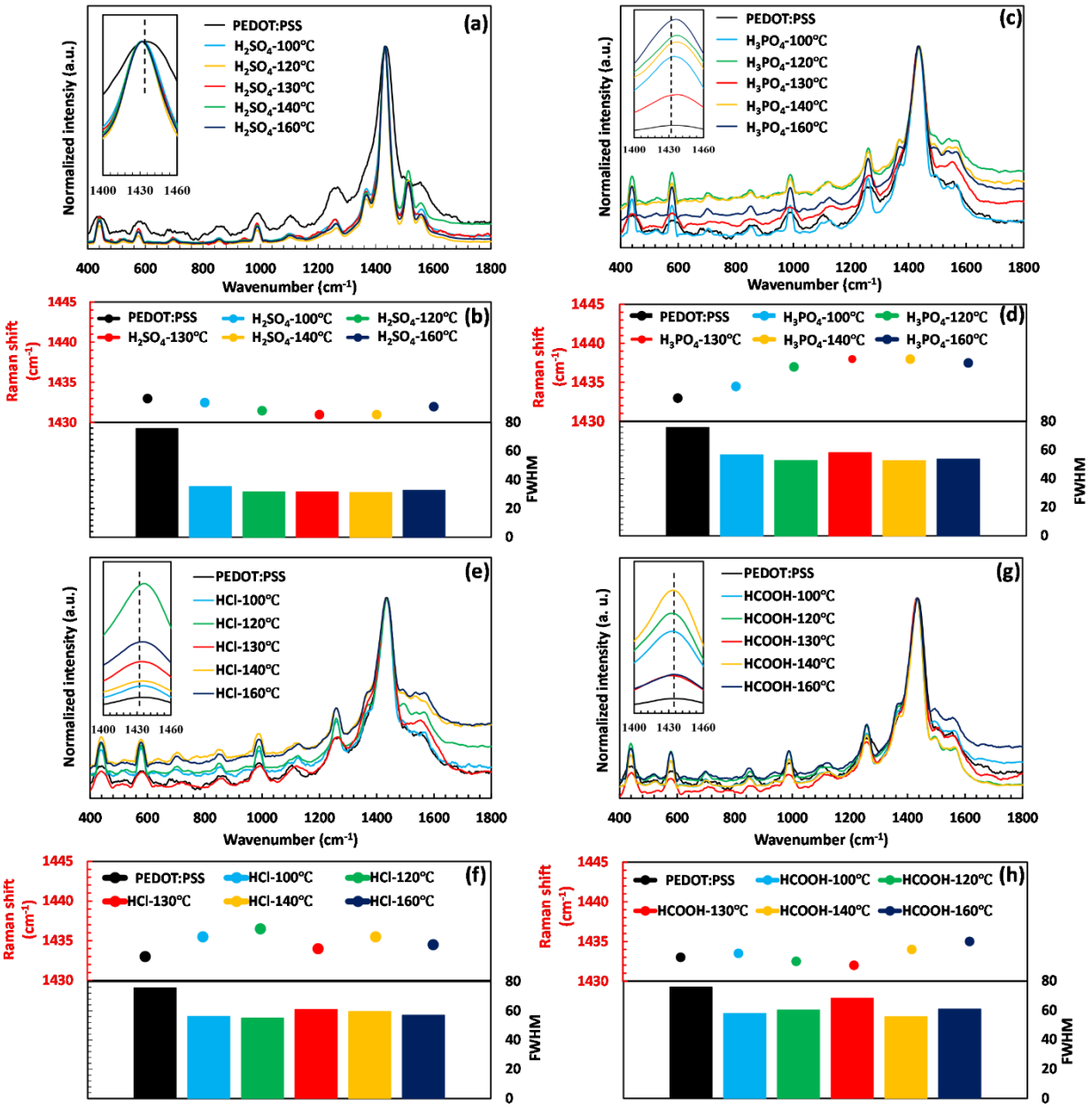

Fig. S3 Raman analysis of PEDOT:PSS treated at different annealing temperatures with a-b) H_2SO_4, c-d) H_3PO_4, e-f) HCl, and g-h) HCOOH. It should be noted the Raman peak shift and FWHM values are attributed to the symmetric $C_\alpha = C_\alpha$ peak.

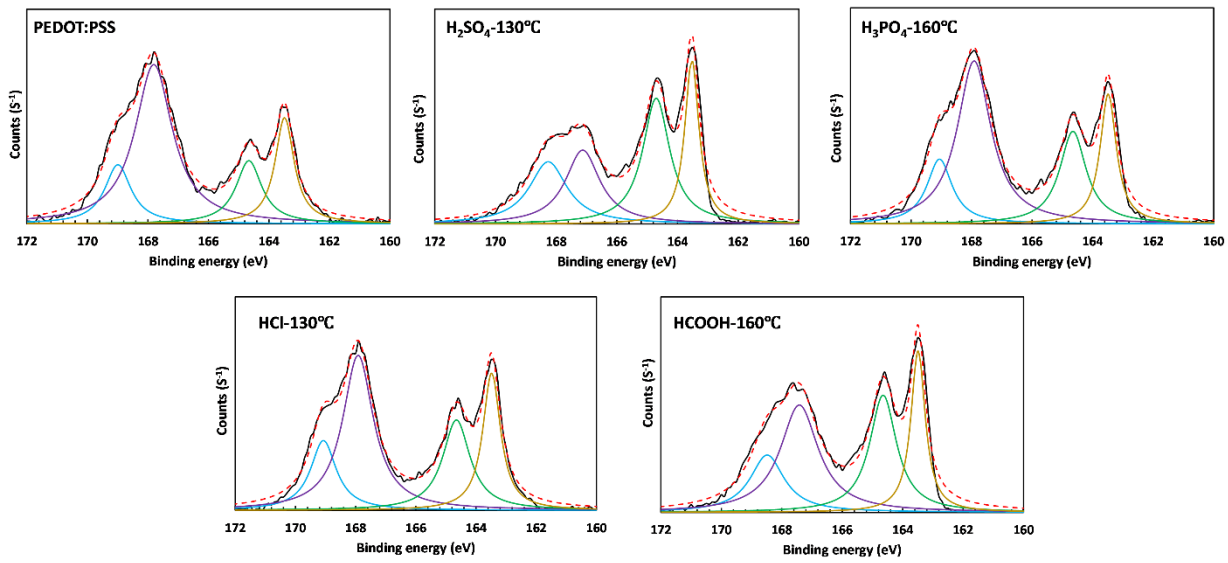

Fig. S4 Deconvoluting the S2p XPS scan of pure and acid-treated PEDOT:PSS films using the Gaussian method.

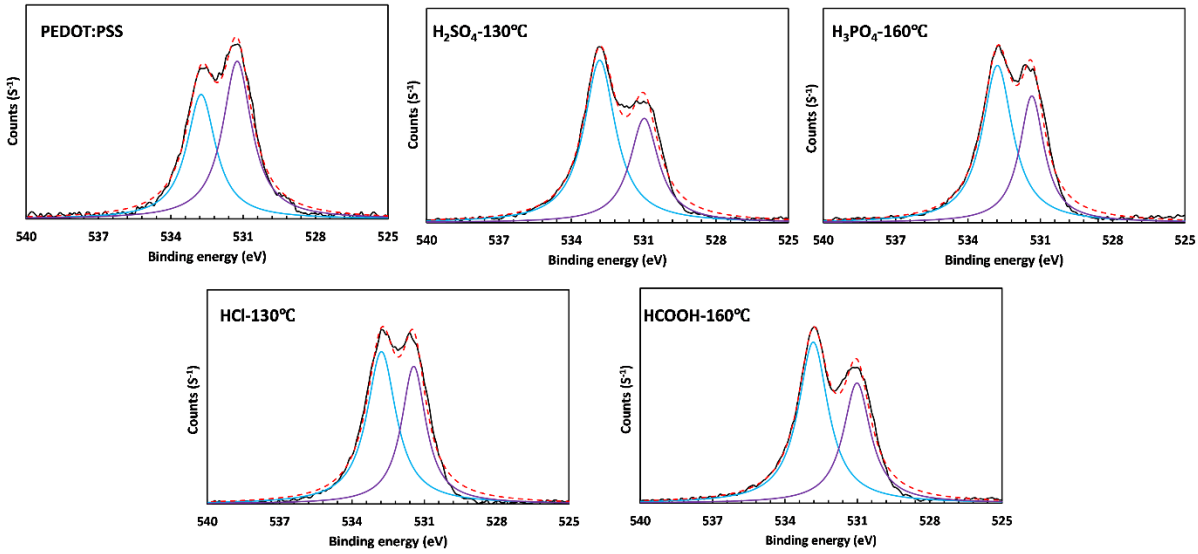

Fig. S5 Deconvoluting the O1s XPS scan of pure and acid-treated PEDOT:PSS films using the Gaussian method.

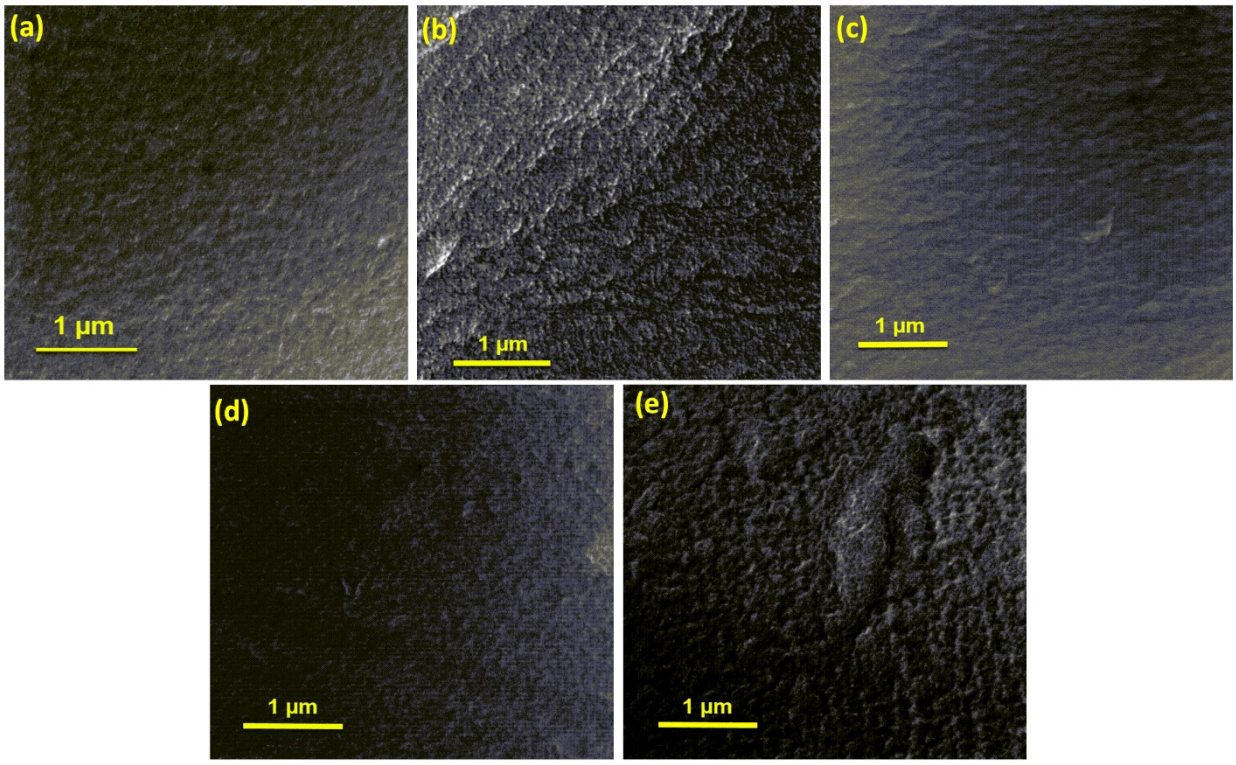

Fig. S6 Surface FESEM images of a) pristine, b) H_2SO_4, c) H_3PO_4, d) HCl, and e) HCOOH treated PEDOT:PSS films.

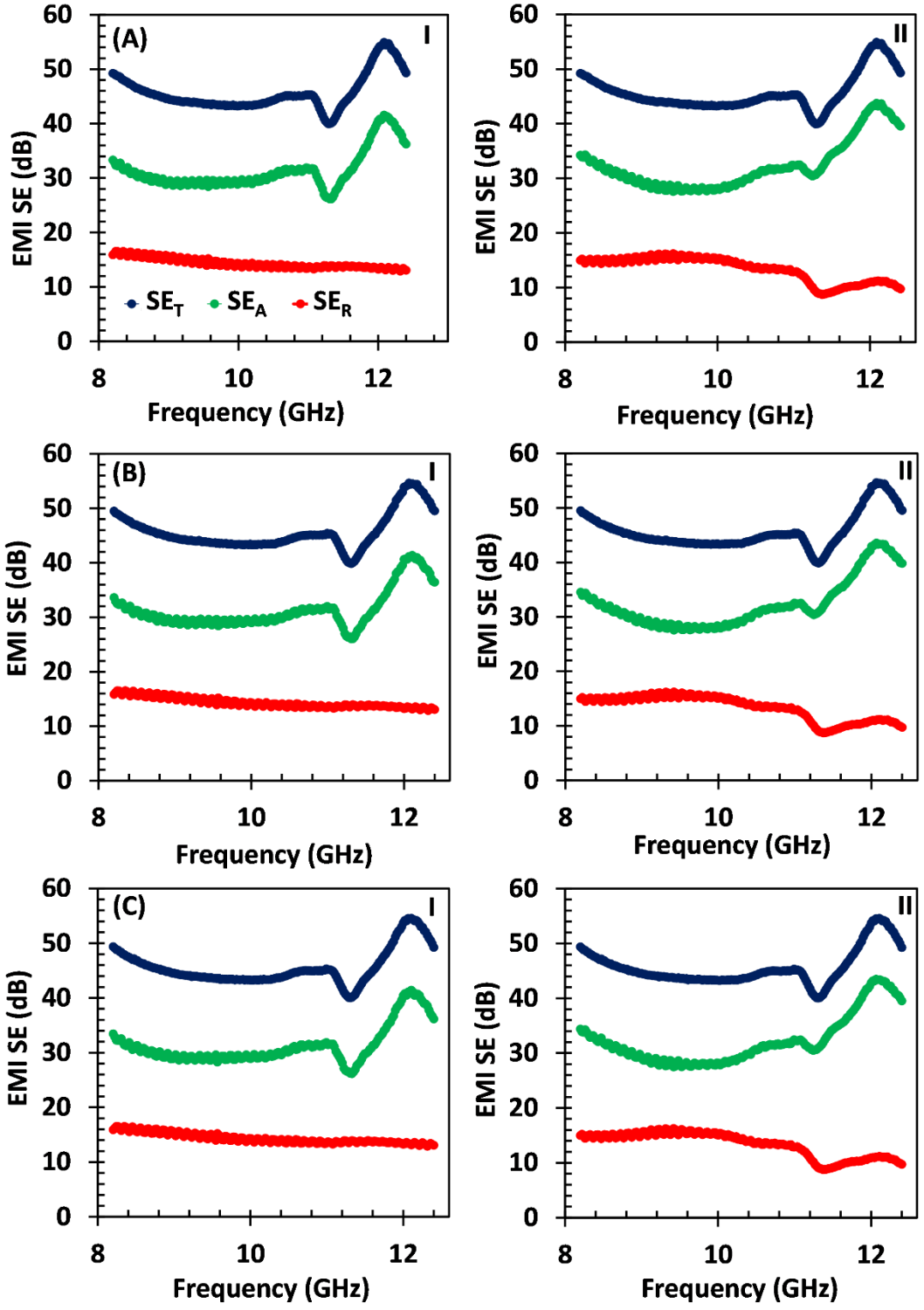

Fig. S7 a-c) EMI shielding characteristics (SE_T, SE_A, SE_R) of the H_2SO_4-treated PEDOT:PSS film. Each sample was tested three times to ensure repeatability. (I) and (II) refer to data collected from ports one and two of the VNA setup, respectively.

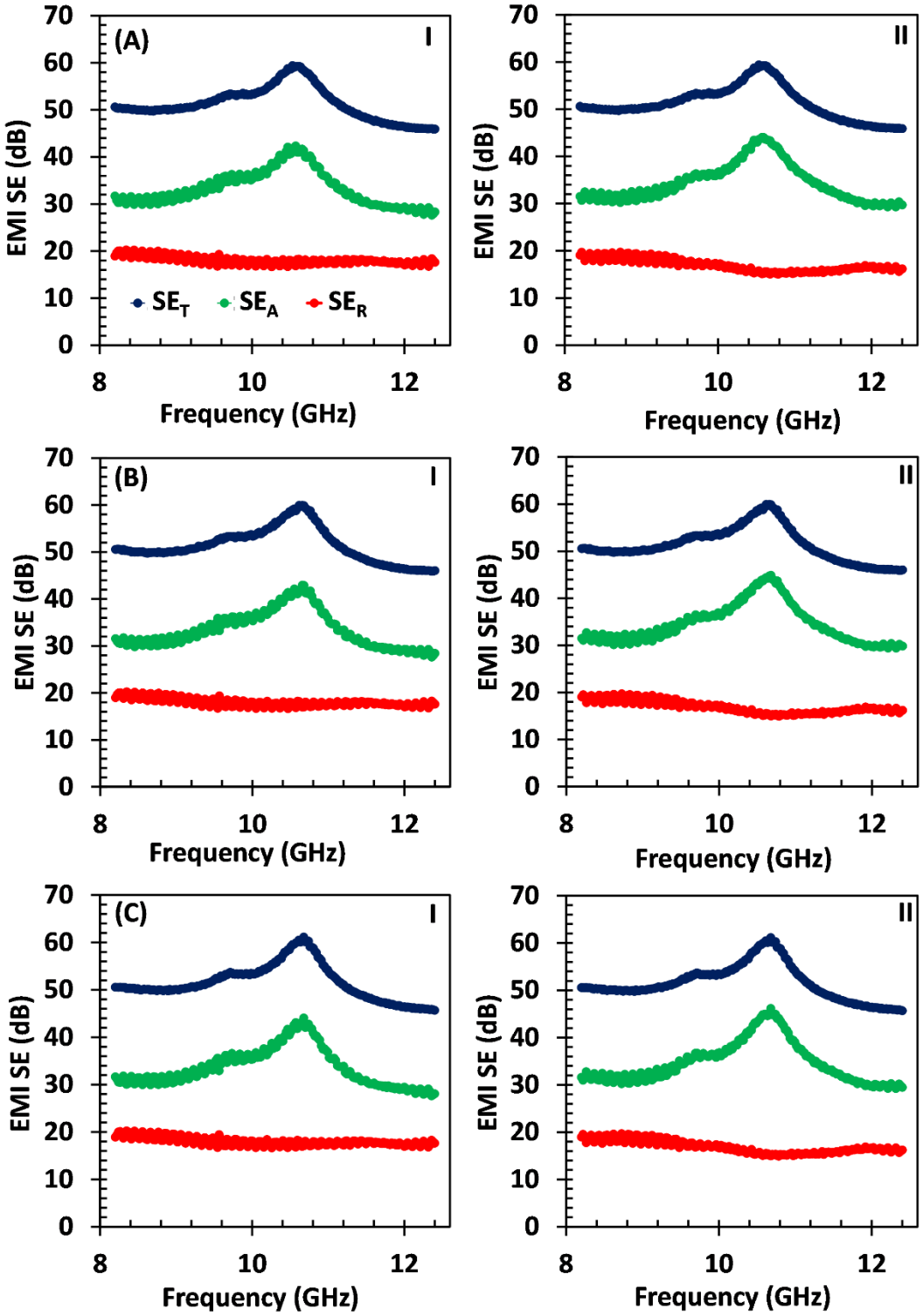

Fig. S8 a-c) EMI shielding characteristics (SE_T, SE_A, SE_R) of hot-pressed H_2SO_4-treated PEDOT:PSS film. Each sample was tested for three times to ensure repeatability. (I) and (II) refer to data collected from ports one and two of the VNA setup, respectively.

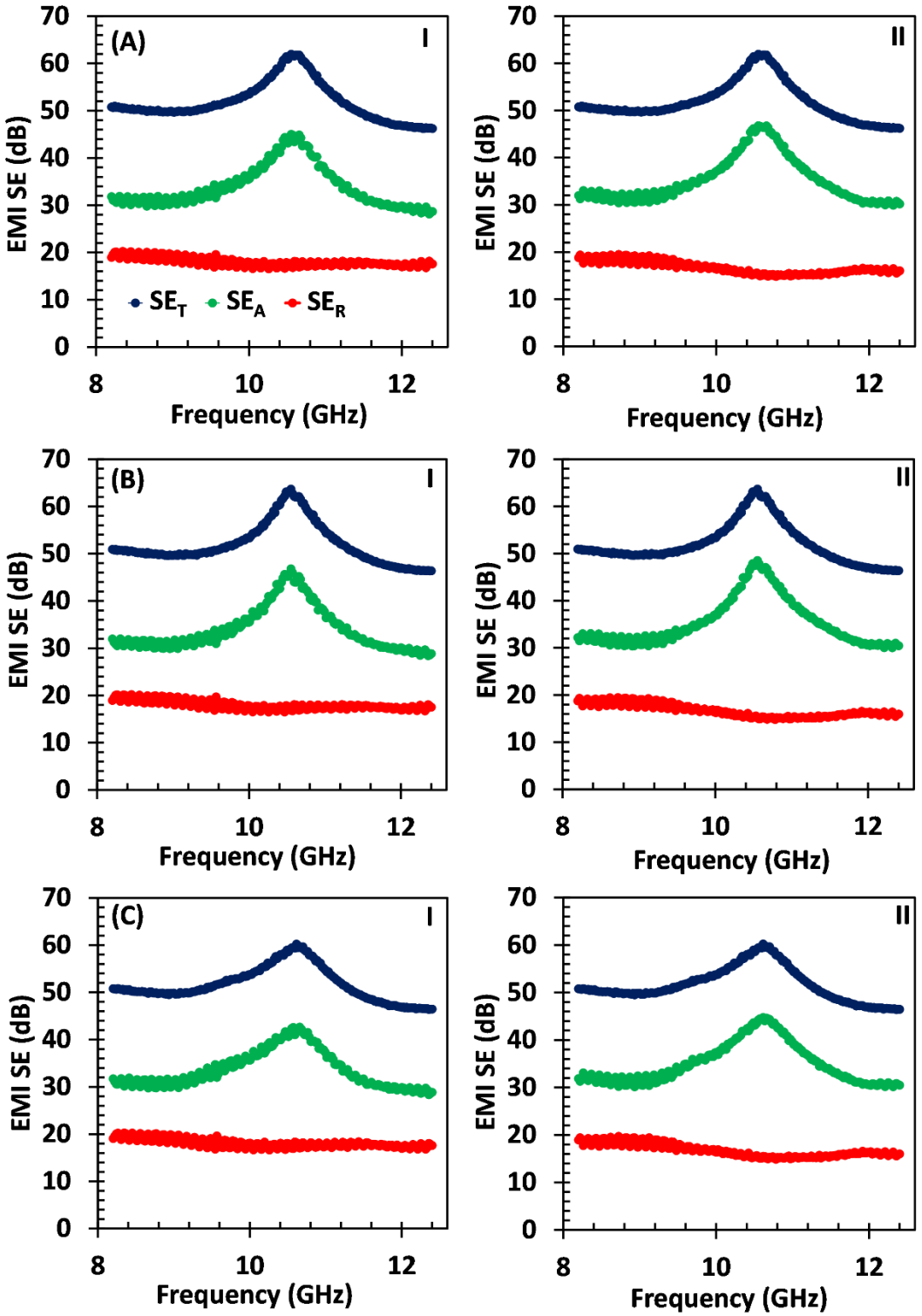

Fig. S9 a-c) EMI shielding characteristics (SE_T, SE_A, SE_R) of hot-pressed H_2SO_4-treated PEDOT:PSS film after 2000 bending cycles. Each sample was tested for three times to ensure repeatability. (I) and (II) refer to data collected from ports one and two of the VNA setup, respectively.

4. Tables

Table S1. FTIR band assignment of pristine and H_2SO_4 treated PEDOT:PSS film.

	Sulfuric acid post-treatment					
Moiety	**Pure PEDOT:PSS (cm^{-1})**	**PEDOT:PSS /H_2SO_4 - 100°C (cm^{-1})**	**PEDOT:PSS/H_2SO_4 - 120°C (cm^{-1})**	**PEDOT:PSS/H_2SO_4- 130°C (cm^{-1})**	**PEDOT:PSS /H_2SO_4 - 140°C (cm^{-1})**	**PEDOT:PSS /H_2SO_4 - 160°C (cm^{-1})**
$C-S$	709	716	718	718	720	718
	853	867	864	864	868	866
	937	925	930	936	925	935
$S-phenyl$	1060	1060	1064	1062	1066	1064
$-SO_3^-$ symmetric	1125	1121	1122	1122	1119	1121
$-SO_3^-$ asymmetric	1158	1162	1165	1164	1164	1164
$C-C$	1261	1274	1266	1266	1267	1266
$C=C$	1543	1423	1543	1545	1538	1539

Table S2. FTIR band assignment of pristine and H_3PO_4 treated PEDOT:PSS film.

	Phosphoric acid post-treatment					
Moiety	**Pure PEDOT:PSS (cm^{-1})**	**PEDOT:PSS /H_3PO_4 - 100°C (cm^{-1})**	**PEDOT:PSS /H_3PO_4 - 120°C (cm^{-1})**	**PEDOT:PSS /H_3PO_4 - 130°C (cm^{-1})**	**PEDOT:PSS /H_3PO_4 - 140°C (cm^{-1})**	**PEDOT:PSS /H_3PO_4 - 160°C (cm^{-1})**
$C-S$	709	716	715	715	715	716
	853	856	857	856	846	855
	937	933	936	936	936	922
$S-phenyl$	1060	1061	1062	1061	1062	1061
$-SO_3^-$ symmetric	1125	1124	1124	1125	1124	1124
$-SO_3^-$ symmetric	1158	1161	1161	1160	1160	1160
$C-C$	1261	1264	1263	1264	1264	1264
$C=C$	1543	1546	1546	1548	1547	1545

Table S3. FTIR band assignment of pristine and HCl treated PEDOT:PSS film.

	Hydrochloric acid post-treatment					
Moiety	**Pure PEDOT:PSS (cm^{-1})**	**PEDOT:PSS /HCl - 100°C (cm^{-1})**	**PEDOT:PSS /HCl - 120°C (cm^{-1})**	**PEDOT:PSS /HCl - 130°C (cm^{-1})**	**PEDOT:PSS /HCl - 140°C (cm^{-1})**	**PEDOT:PSS /HCl - 160°C (cm^{-1})**
$C-S$	709	716	717	720	715	716
	853	854	857	857	856	856
	937	935	940	928	927	920
$S-phenyl$	1060	1061	1057	1057	1062	1063
$-SO_3^-$ symmetric	1125	1126	1134	1134	1124	1124
$-SO_3^-$ asymmetric	1158	1163	1160	1161	1160	1163
$C-C$	1261	1265	1263	1262	1264	1265
$C=C$	1543	1546	1547	1542	1547	1546

Table S4. FTIR band assignment of pristine and HCOOH treated PEDOT:PSS film.

Moiety	Formic acid post-treatment					
	Pure PEDOT:PSS (cm^{-1})	**PEDOT:PSS/ HCOOH - 100℃ (cm^{-1})**	**PEDOT:PSS /HCOOH - 120℃ (cm^{-1})**	**PEDOT:PSS /HCOOH - 130℃ (cm^{-1})**	**PEDOT:PSS /HCOOH - 140℃ (cm^{-1})**	**PEDOT:PSS /HCOOH - 160℃ (cm^{-1})**
$C-S$	709	717	713	714	715	715
	853	855	854	855	854	854
	937	929	935	927	926	932
$S-phenyl$	1060	1063	1063	1063	1062	1063
$-SO_3^-$ symmetric	1125	1122	1121	1123	1123	1123
$-SO_3^-$ asymmetric	1158	1163	1163	1163	1163	1163
$C-C$	1261	1264	1262	1264	1264	1263
$C=C$	1543	1544	1544	1542	1542	1544

Table S5. Binding energy of S2p and O1s contribution for PEDOT and PSS.

	S2p		**O1s**	
	PEDOT	**PSS**	**PEDOT**	**PSS**
PEDOT:PSS	163.43	167.8	532.50	531.00
PEDOT:PSS/H_2SO_4-130℃	163.50	167.00	532.80	531.20
PEDOT:PSS/H_3PO_4-160℃	163.42	167.90	532.70	531.60
PEDOT:PSS/HCl-130℃	163.42	167.80	532.80	531.60
PEDOT:PSS/HCOOH -160℃	163.45	167.36	532.80	531.20

Table S6. XRD peak results for pristine PEDT:PSS and acid post-treated samples.

Index	**PEDOT:PSS**		**PEDOT:PSS/H_2SO_4 - 130℃**		**PEDOT:PSS/H_3PO_4 - 160℃**		**PEDOT:PSS/HCl - 130℃**		**PEDOT:PSS/HCOOH - 160℃**		**PEDOT:PSS/H_2SO_4-130℃ - 50 MPa**	
	2θ	d (Å)	2θ	d (Å)	2θ	d (Å)	2θ	d (Å)	2θ	d (Å)	2θ	d (Å)
d_{100}	7.3	12.1	6.4	13.8	7.1	12.44	7.3	12.1	7	12.71	6.6	13.38
d_{200}	-	-	12.4	7.13	10.1	8.75	10.5	8.42	11	8.04	12.6	7.02
d_{001}	18.1	4.9	19.2	4.62	18.5	4.79	18.5	4.79	18.7	4.75	19.2	4.62
d_{010}	25.9	3.44	25.8	3.45	26.1	3.41	26.3	3.39	25.9	3.44	25.9	3.44

Table S7. GIWAXS peak results for pristine PEDOT:PSS and acid post-treated samples along the out-of-plane direction.

Index	**PEDOT:PSS**		**PEDOT:PSS/H_2SO_4 - 130℃**		**PEDOT:PSS/H_3PO_4 - 160℃**		**PEDOT:PSS/HCl - 130℃**		**PEDOT:PSS/HCOOH - 160℃**		**PEDOT:PSS/H_2SO_4-130℃ - 50 MPa**	
	q($Å^{-1}$)	d (Å)	q($Å^{-1}$)	d (Å)	q($Å^{-1}$)	d (Å)	q($Å^{-1}$)	d (Å)	q($Å^{-1}$)	d (Å)	q($Å^{-1}$)	d (Å)
d_{100}	0.50	12.57	0.42	14.61	0.51	12.32	0.50	12.57	0.52	12.08	0.45	13.65
d_{200}	-	-	0.85	7.39	0.73	8.61	0.74	8.49	0.79	8.05	0.87	7.22
d_{001}	1.29	4.91	1.32	4.76	1.27	4.95	1.30	4.87	1.30	4.83	1.32	4.76

d_{010}	1.84	3.41	1.83	3.43	1.83	3.43	1.84	3.41	1.84	3.39	1.83	3.43

Table S8. GIWAXS peak results for pristine PEDOT:PSS and acid post-treated samples along the in-plane direction.

Index	PEDOT:PSS		PEDOT:PSS/H_2SO_4 - 130°C		PEDOT:PSS/H_3PO_4 - 160°C		PEDOT:PSS/HCl - 130°C		PEDOT:PSS/HCOOH - 160°C		PEDOT:PSS/H_2SO_4-130°C - 50 MPa	
	q($Å^{-1}$)	d (Å)	q($Å^{-1}$)	d (Å)	q($Å^{-1}$)	d (Å)	q($Å^{-1}$)	d (Å)	q($Å^{-1}$)	d (Å)	q($Å^{-1}$)	d (Å)
d_{001}	1.27	4.95	1.20	5.23	1.23	5.12	1.24	5.07	1.25	5.03	1.22	5.15
d_{010}	1.82	3.45	1.86	3.38	1.83	3.43	1.83	3.41	1.86	3.38	1.86	3.38

Table S9. The tensile test results.

	Tensile strength (MPa)	Young modulus (GPa)	Elongation (%)
PEDOT:PSS	46.2	4.8	5.2
PEDOT:PSS/H_2SO_4-130°C	52.5	8.8	2.8
PEDOT:PSS/H_2SO_4-130°C - 50MPa	42.0	19.1	1.4

Table S10. A comparison of the shielding characteristic of developed micrometer-thick PEDOT:PSS shield with previous practices in the literature.

Shield Composition	Thickness (mm)	Conductivity ($S.cm^{-1}$)	SE_T (dB)	SEE/t ($dB\ cm^2\ g^{-1}$)	Ref.
PEDOT:PSS-$Ti_3C_2T_x$	0.011	340.5	42.1	19,498	[3]
PEDOT:PSS-$Ti_3C_2T_x$	0.007	2900±400	55.42	38,079	[4]
PEDOT:PSS-Graphene	0.8	6.84	70	841	[5]
CNF-$Ti_3C_2T_x$	0.035	1.43	39.6	7029	[6]
PVA-$Ti_3C_2T_x$	0.1	2×10^{-4}	26	5136	[7]
PVA-$Ti_3C_2T_x$	0.027	7.16	44.4	9343	[8]
PAN-$Ti_3C_2T_x$-TiO_2	0.045	92.68	32	4085	[9]
ANF-$Ti_3C_2T_x$	0.012	-	34.71	21,971	[10]
CNF-$Ti_3C_2T_x$-AgNW	0.035	373.78	59.7	10,647	[11]
CNF-$Ti_3C_2T_x$	0.047	7.39	24	2647	[12]
PANi-$Ti_3C_2T_x$	0.376	3.25	35.3	1700	[13]
Xanthan-$Ti_3C_2T_x$	0.00684	115.29	34.1	14,490	[14]
Epoxy-$Ti_3C_2T_x$-rGO	2	6.95	56.4	9400	[15]
POM-MWCNT	2	3.33	58.6	344.4	[16]
PC-MWCNT	2.16	3	39	164	[17]
PVDF-MWCNT	0.9	0.074	32	259	[18]
PS-Graphene	2.5	1.25	29	322	[19]
PHBV-AgNW	0.018	-	45.9	19.678	[20]
PMMA-Graphene	0.24	3.11	19	1042	[21]
Neat $Ti_3C_2T_x$	0.014	-	38.33	42932	[2]

80 wt% $Ti_3C_2T_x$	0.021	-	28.06	32240	[2]
50 wt% $Ti_3C_2T_x$	0.024	-	16.26	20246	[2]
H_2SO_4-treated hot-pressed PEDOT:PSS	0.0046	3360	51.79	75,057.97	This work

Abbreviations: Poly(3,4-ethylenedioxythiophene):polystyrene sulfonate (PEDOT:PSS), cellulose nanofiber (CNF), polyvinyl alcohol (PVA), polyacrylonitrile (PAN), Aramid nanofiber (ANF), nanocellulose (NC), polyaniline (PANi), reduced graphene oxide (rGO), Poly(oxymethylene) (POM), multi-walled carbon nanotube (MWCNT), polycarbonate (PC), polvinylidene fluoride (PVDF), polystyrene (PS), poly(3-hydrobutyrate-co-3-hydroxyvalerate) (PHBV), silver nanowire (AgNW), polymethyl methacrylate (PMMA).

Reference

1. J. Dong and G. Portale, *Advanced Materials Interfaces*, 2020, **7**, 2000641.
2. A. Ghaffarkhah, M. Kamkar, Z. A. Dijvejin, H. Riazi, S. Ghaderi, K. Golovin, M. Soroush and M. Arjmand, *Carbon*, 2022, **191**, 277-289.
3. R. Liu, M. Miao, Y. Li, J. Zhang, S. Cao and X. Feng, *ACS Applied Materials & Interfaces*, 2018, **10**, 44787-44795.
4. A. Ghaffarkhah, M. Kamkar, H. Riazi, E. Hosseini, Z. A. Dijvejin, K. Golovin, M. Soroush and M. Arjmand, *New Journal of Chemistry*, 2021, **45**, 20787-20799.
5. N. Agnihotri, K. Chakrabarti and A. De, *RSC Advances*, 2015, **5**, 43765-43771.
6. B. Zhou, Z. Zhang, Y. Li, G. Han, Y. Feng, B. Wang, D. Zhang, J. Ma and C. Liu, *ACS Applied Materials & Interfaces*, 2020, **12**, 4895-4905.
7. H. Xu, X. Yin, X. Li, M. Li, S. Liang, L. Zhang and L. Cheng, *ACS Applied Materials & Interfaces*, 2019, **11**, 10198-10207.
8. X. Jin, J. Wang, L. Dai, X. Liu, L. Li, Y. Yang, Y. Cao, W. Wang, H. Wu and S. Guo, *Chemical Engineering Journal*, 2020, **380**, 122475.
9. Y. Wang, H.-K. Peng, T.-T. Li, B.-C. Shiu, H.-T. Ren, X. Zhang, C.-W. Lou and J.-H. Lin, *Chemical Engineering Journal*, 2021, **412**, 128681.
10. H. Wei, M. Wang, W. Zheng, Z. Jiang and Y. Huang, *Ceramics International*, 2020, **46**, 6199-6204.
11. B. Zhou, Q. Li, P. Xu, Y. Feng, J. Ma, C. Liu and C. Shen, *Nanoscale*, 2021, **13**, 2378-2388.
12. W.-T. Cao, F.-F. Chen, Y.-J. Zhu, Y.-G. Zhang, Y.-Y. Jiang, M.-G. Ma and F. Chen, *ACS Nano*, 2018, **12**, 4583-4593.

13. G. Yin, Y. Wang, W. Wang, Z. Qu and D. Yu, *Advanced Materials Interfaces*, 2021, **8**, 2001893.
14. Y. Sun, R. Ding, S. Y. Hong, J. Lee, Y.-K. Seo, J.-D. Nam and J. Suhr, *Chemical Engineering Journal*, 2021, **410**, 128348.
15. D. Liu, H.-J. Li, J. Gao, S. Zhao, Y. Zhu, P. Wang, D. Wang, A. Chen, X. Wang and J. Yang, *Nanoscale Research Letters*, 2018, **13**, 261.
16. J. Li, J.-L. Chen, X.-H. Tang, J.-H. Cai, J.-H. Liu and M. Wang, *Journal of Colloid and Interface Science*, 2020, **565**, 536-545.
17. S. Pande, A. Chaudhary, D. Patel, B. P. Singh and R. B. Mathur, *RSC Advances*, 2014, **4**, 13839-13849.
18. B. Bhaskara Rao, N. Kale, B. Kothavale and S. Kale, *AIP Advances*, 2016, **6**, 065107.
19. D.-X. Yan, P.-G. Ren, H. Pang, Q. Fu, M.-B. Yang and Z.-M. Li, *Journal of Materials Chemistry*, 2012, **22**, 18772-18774.
20. S. Yang, Y.-Y. Wang, Y.-N. Song, L.-C. Jia, G.-J. Zhong, L. Xu, D.-X. Yan, J. Lei and Z.-M. Li, *Journal of Materials Chemistry C*, 2021, **9**, 3307-3315.
21. H.-B. Zhang, Q. Yan, W.-G. Zheng, Z. He and Z.-Z. Yu, *ACS Applied Materials & Interfaces*, 2011, **3**, 918-924.